Separation Science and Technology
Publication details, including instructions for authors and subscription information:
http://www.informaworld.com/smpp/title~content=t713708471

Soil Cleanup by In-Situ Aeration. XVIII. Field-Scale Models with Diffusion from Clay Structures

José M. Rodríguez-Maroto[a]; César Gómez-Lahoz[a]; David J. Wilson[ab]
[a] DEPARTMENT DE INGENIERíA QUíMICA FACULTAD DE CIENCIAS CAMPUS UNIVERSITIARIO DE TEATINOS UNIVERSIDAD, DE MÁLAGA, MÁLAGA, SPAIN [b] Department of Chemistry, Vanderbilt University, Nashville, Tennessee, USA

To cite this Article Rodríguez-Maroto, José M. , Gómez-Lahoz, César and Wilson, David J.(1994) 'Soil Cleanup by In-Situ Aeration. XVIII. Field-Scale Models with Diffusion from Clay Structures', Separation Science and Technology, 29: 11, 1367 — 1399
To link to this Article: DOI: 10.1080/01496399408003027
URL: http://dx.doi.org/10.1080/01496399408003027

SEPARATION SCIENCE AND TECHNOLOGY, **29**(11), pp. 1367–1399, 1994

Soil Cleanup by In-Situ Aeration. XVIII. Field-Scale Models with Diffusion from Clay Structures

JOSÉ M. RODRÍGUEZ-MAROTO, CÉSAR GÓMEZ-LAHOZ, and DAVID J. WILSON*
DEPARTAMENTO DE INGENIERÍA QUÍMICA
FACULTAD DE CIENCIAS
CAMPUS UNIVERSITIARIO DE TEATINOS
UNIVERSIDAD DE MÁLAGA
29071 MÁLAGA, SPAIN

ABSTRACT

Mathematical models for soil vapor extraction (SVE) are developed which model solution of nonaqueous phase liquid (NAPL) and mass transport of volatile organic compounds (VOCs) through low-permeability lumps, lenticular structures, and discontinuous layers of clay by means of a distributed diffusion approach. The well configurations modeled are that of a single buried horizontal slotted pipe and that of a single vertical well screened along a short length near its bottom. The models yield high off-gas VOC concentrations initially, followed typically by vary rapid drop-offs to relatively long plateaus, followed in turn by terminal tailing, the length of which is highly variable and determined by the thickness of the low-permeability layers from which diffusion is occurring and by the size of the NAPL droplets (if NAPL is present). The results are in agreement with a previous, simpler model; they indicate that it will be impossible to accurately predict SVE cleanup times from data taken in short-term pilot-scale experiments removing only 5–25% of the VOC present in the domain of influence of the well.

INTRODUCTION

Soil vapor extraction (SVE) is now well-established for the remediation of sites contaminated with volatile organic compounds (VOCs). Approxi-

* Permanent address: Department of Chemistry, Box 1822, Station B, Vanderbilt University, Nashville, Tennessee 37235, USA.

mately 83 Superfund sites were using or scheduled to use the technique as of October 1992, and it is being used on a large number of other sites involving VOCs. EPA has published a number of reports on SVE (1–4) as well as the proceedings of a symposium on the subject (5). Hutzler and his coworkers (6, 7) and Wilson and Clarke (8) have reviewed the technique in some detail. The literature on the subject is sufficiently extensive that no attempt will be made to provide a complete review here.

Mathematical modeling techniques for SVE provide support for initial site-specific evaluation, interpretation of lab and pilot-scale field data, design of pilot- and full-scale field SVE facilities, and estimation of costs and cleanup times. Several groups of workers have developed SVE models, including the Vapex group (9–15 and other papers); Johnson, Kemblowski, and their coworkers (16–20 and other papers); Cho (21); the group at the Idaho National Engineering Laboratory (22, 23); and the Eckenfelder–Vanderbilt group (24–26, for example).

The initial hope that the assumption of local equilibrium with respect to movement of VOC between the advecting soil gas and the stationary phase(s) containing VOC would be an adequate approximation (27, 28) has since been dashed at a number of sites. At these, rapid declines in off-gas VOC concentrations after a few days (sometimes only a few hours) of operation and a long-drawn-out period of tailing during the lengthy terminal phase establish that local equilibrium is not being maintained—that diffusion/desorption kinetics are controlling the rate of release of VOC to the advecting vapor phase. DiGiulio et al. (29) described possible pilot-scale field experiments to evaluate mass transport limitations, and Lyman and Noonan (3) indicated that such limitations are common.

Some time ago we described a simple lumped parameter method for including mass transport limitations in SVE models which could give removal rates greatly reduced below those from models in which local equilibrium was assumed (30–33). This model, however, could not yield with the same parameter set the very rapid initial VOC removal rates and the quite slow removal rates toward the end of the remediation which are observed experimentally. It was evident that a model which provided a richer spectrum of time constants for mass transport would be necessary.

This difficulty was discussed recently (34), and a lab column model was described which employs a more realistic approach to diffusion transport. This was one of two models investigated. These distributed diffusion models assume that VOC diffuses from water-saturated layers of finite thickness before it reaches the advecting soil gas and is removed. In one approach the NAPL is present as droplets distributed throughout the water-saturated low-porosity layers; in the other the NAPL is present as

a film within the water-saturated lamellae. The two approaches could be made to yield rather similar results on suitable selection of the parameters in the models. The second model requires substantially less than half the computer time required by the first. It also permits use of steady-state approximations which can greatly speed the computations.

In the last paper of this series (35) we discussed the extension of the second approach (in which NAPL is present as a thin layer within the low-permeability lenticular domains from which it must diffuse to the advecting air) to SVE by means of a horizontal slotted pipe well. The model performed well, easily producing the high initial VOC removal rates, the rapid declines in off-gas VOC concentration, and the lengthy plateaus and tailing observed experimentally. Computationally, the model could easily be run on a 386 NX microcomputer (with a math coprocessor) at 20 MHz, and the steady-state approximations provided substantial increases in speed of computation with no loss of accuracy.

We felt somewhat uneasy about the artificiality of the model, however. It was difficult to see how the postulated thin layer of NAPL was to be created deep within the low permeability structures in the first place. This left the model of the diffusion process lacking the sort of easily visualized physicochemical foundation which one would like. It had some meaning in terms of the least dimension of the low-permeability structures, and it seemed to produce quite reasonable results, but it also seemed rather contrived. We felt much more comfortable about the model in which the NAPL was distributed as droplets throughout the low-permeability structures, but previous work (34) on a one-dimensional model of this type had made it clear that the computational demands of a two-dimensional version were beyond the capabilities of our microcomputers.

The arrival of a 50-MHz 486 DX microcomputer just as that project was being completed changed the situation; this was a feasible machine for the development and use of a two-dimensional distributed NAPL droplet model for SVE. In the following sections we present two versions of such a model, one for SVE with a buried horizontal slotted pipe, and one for SVE with a single vertical well screened for a short distance along its bottom. The analysis is done first for the horizontal slotted pipe configuration, then for the single vertical well. This is followed by a section in which results of computations done with the two versions are presented and discussed. The paper closes with a short section on conclusions.

ANALYSIS

The configuration of the horizontal slotted pipe SVE well is shown in Fig. 1, along with much of the notation. The model for diffusion transport,

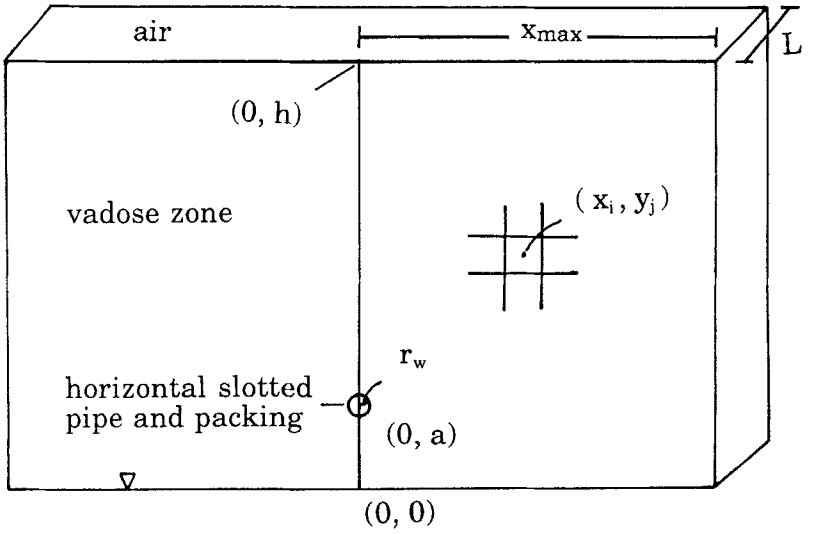

FIG. 1 SVE well, buried horizontal slotted pipe configuration; geometry and notation.

together with notation, is shown in Fig. 2. The development of an SVE model breaks down into three major parts; the calculation of the soil gas flow field in the vicinity of the vacuum well, the analysis of the equilibria and mass transport factors governing the release of the VOC being vapor stripped, and the combining of the two to form the model.

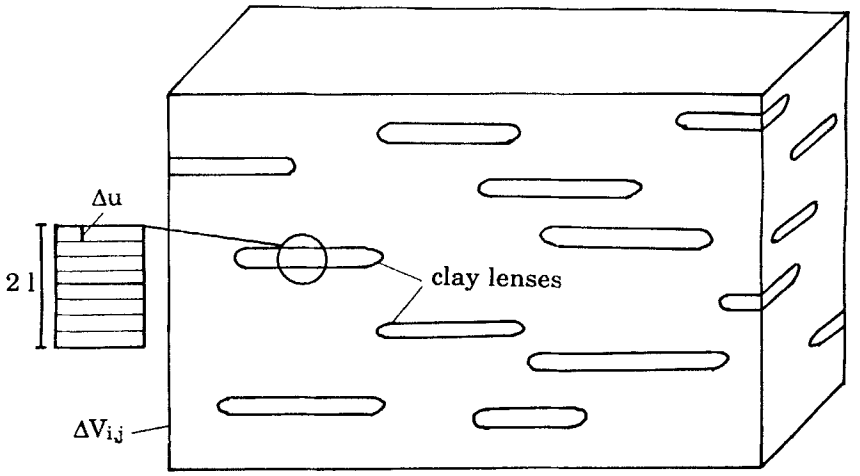

FIG. 2 Model for solution kinetics of NAPL and diffusion transport of dissolved VOC.

I. Model for SVE by Means of a Single Long Horizontal Slotted Pipe

A. Gas Flow Field

We shall assume a porous medium of constant, isotropic permeability, so that we may use the method of images from electrostatics (36) for calculating the soil gas pressures in the vicinity of the SVE well. We shall model only the right side of the domain, since from symmetry the left is a mirror image of the right, and we shall neglect effects at the ends of the pipe. We work in Cartesian coordinates x, y. Let

h = thickness of porous medium (depth to water table), m
x_{max} = half-width of domain of interest (at right angles to the axis of the SVE pipe), m
L = length of horizontal slotted SVE pipe, m
r_w = radius of gravel packing of the horizontal slotted pipe, m
P_w = wellhead gas pressure (<1 atm), atm
P_a = ambient pressure, atm
$P(x, y)$ = soil gas pressure at the point (x, y), atm
K_D = Darcy's constant, $m^2/atm \cdot s$
a = distance of well above the water table, m
Q = molar gas flow rate to well, mol/s
q = standard volumetric gas flow rate to well, m^3/s
v_x = x-component of superficial velocity, m/s ($m^3/m^2 \cdot s$)
v_y = y-component of superficial velocity, m/s ($m^3/m^2 \cdot s$)
R = gas constant, 8.206×10^{-5} $m^3 \cdot atm/mol \cdot deg$
T = temperature, degrees Kelvin

The pressure of an ideal gas in a porous medium satisfies the equation

$$\nabla^2 P^2 = 0 \tag{1}$$

The solution to this equation must satisfy the boundary conditions

$$\frac{\partial P^2(x, 0)}{\partial y} = 0 \tag{2}$$

at the water table and

$$P^2(x, h) = 1 \text{ (atm)}^2 \tag{3}$$

at the soil surface. See Fig. 1. Also, a sink to represent the vacuum well is needed at $(0, a)$.

The velocity potential is defined as

$$W(x, y) + P_a^2 = P^2(x, y) \tag{4}$$

so that the problem becomes

$$\nabla^2 W = 0 \tag{5}$$

$$\frac{\partial W(x, 0)}{\partial y} = 0 \tag{6}$$

$$W(x, h) = 0 \tag{7}$$

The following expression for W can be shown by symmetry arguments to satisfy the necessary boundary conditions, and has a sink at $(0, a)$.

$$\begin{aligned} W = B \sum_{n=-\infty}^{\infty} & [\log\{x^2 + (y - 4nh - a)^2\} \\ & + \log\{x^2 + [y - 4nh + a]^2\} \\ & - \log\{x^2 + [y - (4n - 2)h - a]^2\} \\ & - \log\{x^2 + [y - (4n - 2)h + a]^2\}] \end{aligned} \tag{8}$$

Since the wellhead pressure is given (P_w), we have

$$P^2(r_w, a) = P_w^2$$

which gives, after a little rearranging,

$$\begin{aligned} P_a^2 - P_w^2 = & -B \sum_{n=-\infty}^{\infty} [\log_e\{r_w^2 + [-4nh]^2\} \\ & + \log_e\{r_w^2 + [2a - 4nh]^2\} \\ & - \log_e\{r_w^2 + [-(4n - 2)h]^2\} \\ & - \log_e(\{r_w^2 + [2a - (4n - 2)h]^2\}] \\ = & -BU \end{aligned} \tag{9}$$

where U is the sum in Eq. (9). B is therefore given by

$$B = -(P_a^2 - P_w^2)/U \tag{10}$$

The molar gas flow rate is given by

$$Q = LK_D \int_0^{2\pi} (P/RT)(\nabla_r P) r d\theta \tag{11}$$

where r is the radial coordinate in cylindrical coordinates centered at the pipe, and θ is the angular coordinate. K_D is Darcy's constant, and we have assumed that the superficial gas velocity is given by Darcy's law,

$$v = -K_D \nabla P \tag{12}$$

Note that $P\nabla_r P = (1/2)\nabla_r(P^2) = (1/2)\nabla_r W$.

From Eq. (8) we see that

$$W = B \log_e r^2 + \text{terms regular as } r \to 0 \tag{13}$$

The regular terms contribute nothing to the integral (Eq. 11) if the surface of integration encloses only the singularity at $r = 0$. We then obtain

$$RTQ = q = 2\pi L K_D B \tag{14}$$

and

$$B = q/(2\pi L K_D) \tag{15}$$

Setting Eqs. (10) and (15) equal and solving for K_D then gives

$$K_D = -\frac{qU}{2\pi L(P_a^2 - P_w^2)} \tag{16}$$

for Darcy's constant.

Then, since $W + P_a^2 = P^2$,

$$\nabla W = 2P\nabla P \tag{17}$$

and

$$\nabla P = \nabla W/(2P) = \frac{\nabla W}{2[W + P_a^2]^{1/2}} \tag{18}$$

then provides the components of the pressure gradient. Use of Eq. (18) in Eq. (12) then gives

$$v = -\frac{K_D \nabla W}{2[W + P_a^2]^{1/2}} \tag{19}$$

B. The Advection Terms

We are now in position to calculate the advection terms in the mass balance equations for VOC in the gas phase in the volume elements into which the system will be partitioned for analysis. We obtain for the advection contribution to this mass balance the following:

$$\begin{aligned} \sigma \Delta x \Delta y L \left[\frac{dC_{ij}^g}{dt}\right]_{\text{adv}} &= L\Delta y v_{ij}^{\text{L}}[S(v^{\text{L}})C_{i-1,j}^g + S(-v^{\text{L}})C_{ij}^g] \\ &+ L\Delta y v_{ij}^{\text{R}}[-S(-v^{\text{R}})C_{i+1,j}^g - S(v^{\text{R}})C_{ij}^g] \\ &+ L\Delta x v_{ij}^{\text{B}}[S(v^{\text{B}})C_{ij-1}^g + S(-v^{\text{B}})C_{ij}^g] \\ &+ L\Delta x v_{ij}^{\text{T}}[-S(-v^{\text{T}})C_{ij+1}^g - S(v^{\text{T}})C_{ij}^g] \end{aligned} \tag{20}$$

Here the superscripts L, R, B, and T refer to the left, right, bottom, and top of the volume element, respectively, and σ is the air-filled porosity,

$$\begin{aligned} S(u) &= 1, \; u > 1 \\ &= 0, \; u \leqslant 1 \end{aligned} \tag{21}$$

and $S(v^{\mathrm{L}})$ is an abbreviation for $S(v_{ij}^{\mathrm{L}})$, etc. The velocities are given by

$$v_{ij}^{\mathrm{L}} = v_x[(i - 1)\Delta x, (j - 1/2)\Delta y] \tag{22}$$

$$v_{ij}^{\mathrm{R}} = v_x[i\Delta x, (j - 1/2)\Delta y] \tag{23}$$

$$v_{ij}^{\mathrm{B}} = v_y[(i - 1/2)\Delta x, (j - 1)\Delta y] \tag{24}$$

$$v_{ij}^{\mathrm{T}} = v_y[(i - 1/2)\Delta x, j\Delta y] \tag{25}$$

where v_x and v_y are the components of Eq. (19).

C. The Rate of Solution of Droplets of NAPL

We first look at dissolution of VOC from a NAPL droplet into the aqueous phase. See Fig. 3. The equation for steady-state diffusion from a spherical droplet is

$$\frac{1}{r^2}\frac{d}{dr}\left[r^2\frac{dC}{dr}\right] = 0 \tag{26}$$

with boundary conditions

$$C(a) = C_{\mathrm{sat}} \tag{27}$$

and

$$C(b) = C_0 \tag{28}$$

where C_{sat} is the aqueous solubility of the VOC and C_0 is the VOC concentration at the outer surface ($r = b$) of the aqueous boundary layer surrounding the drop. Equation (26) integrates to

$$C(r) = c_1/r + c_2 \tag{29}$$

Use of the boundary conditions then gives

$$C(r) = \frac{ab}{b - a}(C_{\mathrm{sat}} - C_0)/r + c_2 \tag{30}$$

from which

$$\frac{dC}{dr} = -\frac{ab}{b - a}(C_{\mathrm{sat}} - C_0)/r^2 \tag{31}$$

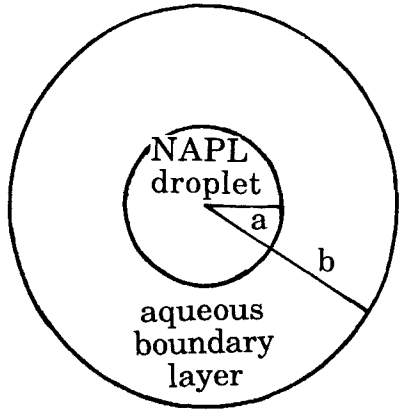

FIG. 3 Solution of a single NAPL droplet.

Fick's first law and Eq. (31) then give for the mass m of the droplet

$$\frac{dm}{dt} = -\frac{4\pi Da(C_{sat} - C_0)}{1 - a/b} \tag{32}$$

It is easily shown that

$$a = a_0(m/m_d)^{1/3} \tag{33}$$

where m_d is the initial mass of the droplet, a_0 is its initial radius, and m and a are values at a later time t. So

$$\frac{dm}{dt} = -\frac{4\pi Da_0(C_{sat} - C_0)(m/m_d)^{1/3}}{1 - (a_0/b)(m/m_d)^{1/3}} \tag{34}$$

A reasonable value for b, the boundary layer thickness around a droplet, is half the average distance between droplets. This is obtained as follows. The number of NAPL droplets in a volume element $L\Delta x\Delta y$ is given by n, where

$$n\frac{4\pi a_0^3\rho_{voc}}{3} = L\Delta x\Delta y C_0^N \tag{35}$$

where ρ_{voc} = VOC density, kg/m^3
C_0^N = initial NAPL concentration, kg/m^3

So

$$n = \frac{3L\Delta x\Delta y C_0^N}{4\pi a_0^3\rho_{voc}} \tag{36}$$

These are contained in a volume of water $\omega L \Delta x \Delta y$, where ω is the water-filled porosity, so the volume of water per droplet is

$$V' = \frac{4\pi\omega\rho_{voc}a_0^3}{3C_0^N} \tag{37}$$

and the mean distance between droplets is then

$$2b = a_0\left[\frac{4\pi\omega\rho_{voc}}{3C_0^N}\right]^{1/3} \tag{38}$$

Finally,

$$b = a_0\left[\frac{\pi\omega\rho_{voc}}{6C_0^N}\right]^{1/3} \tag{39}$$

gives the thickness of the boundary layer.

D. Initial Distribution of VOC among the Phases

This question is addressed as follows. Assume the initial concentrations in the gas, aqueous, and NAPL phases are constant from volume element to volume element and that the aqueous and NAPL phase concentrations are constant from slab to slab within a volume element. See Fig. 4. Then

$$C_{tot} = \sigma C_0^g + \omega C_0^w + C_0^N \tag{40}$$

where C_0^g, C_0^w, and C_0^N are the initial gaseous, aqueous, and NAPL concentrations, respectively. Assume that $C_0^N = 0$ and that the aqueous and gaseous phases are at equilibrium with respect to VOC transport. Then use of Henry's law yields

$$C_0^w = \frac{C_{tot}}{\sigma K_H + \omega} \tag{41}$$

and

$$C_0^g = K_H C_0^w \tag{42}$$

If $C_0^w < C_{sat}$, use these values and set $C_0^N = 0$. If $C_0^w > C_{sat}$, however, then use

$$C_0^w = C_{sat} \tag{43}$$

$$C_0^g = K_H C_{sat} \tag{44}$$

$$C_0^N = C_{tot} - (\sigma K_H + \omega)C_{sat} \tag{45}$$

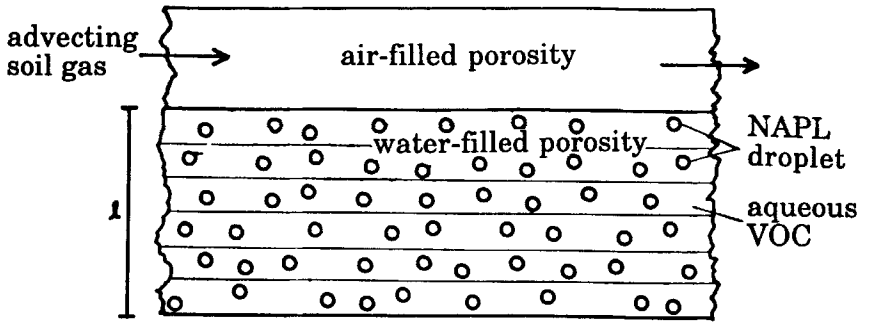

FIG. 4 Slabs used to represent a low-permeability water-saturated lens.

E. Rate of Change of NAPL Mass

Recall that the number of NAPL droplets in a volume element is given by

$$n = \frac{3L\Delta x\Delta y C_0^N}{4\pi a_0^3 \rho_{\text{voc}}} \tag{36'}$$

The number of NAPL droplets in a single slab in a volume element is

$$n' = \frac{n}{n_u} = \frac{3L\Delta x\Delta y C_0^N}{4\pi a_0^3 \rho_{\text{voc}} n_u} \tag{46}$$

The initial mass of NAPL in a single slab is

$$m_0 = L\Delta x\Delta y C_0^N / n_u \tag{47}$$

The initial mass of a droplet, m_d, is

$$m_d = \frac{4\pi a_0^3 \rho_{\text{voc}}}{3} \tag{48}$$

Finally, on using Eq. (34), we find that the mass of NAPL in the kth slab of the ijth volume element is governed by

$$\frac{dm_{ijk}}{dt} = -\frac{3L\Delta x\Delta y C_0^N D(C_{\text{sat}} - C_{ijk}^w)(m_{ijk}/m_0)^{1/3}}{n_u a_0^2 \rho_{\text{voc}}[1 - (a_0/b)(m_{ijk}/m_0)^{1/3}]} \tag{49}$$

F. Change in Aqueous VOC Concentration

Let us assume that the clay lenses from which diffusion is taking place are of thickness $2l$, and that they contain the bulk of the water in the soil.

See Fig. 4. Then the volume of water in a volume element can be written as

$$V_w = \omega L \Delta x \Delta y = 2lA\nu_{clay} \tag{50}$$

where A = total cross-sectional area of saturated clay lenses in the volume element, m^2
ν_{clay} = porosity of the clay

Then

$$A = \frac{\omega L \Delta x \Delta y}{2l\nu_{clay}} \tag{51}$$

and the total area of lenses from which VOC may diffuse (counting top halves and bottom halves separately) is

$$2A = \frac{\omega L \Delta x \Delta y}{l\nu_{clay}} \tag{52}$$

This is also the area of the interface between any two adjacent slabs within the volume element into which the aqueous phase is partitioned and between which diffusion transport of VOC may take place.

A mass balance on the aqueous phase VOC in the kth slab of the ijth volume element then yields

$$\frac{\omega L \Delta x \Delta y}{n_u} \frac{dC^w_{ijk}}{dt} = \frac{\omega L \Delta x \Delta y}{l\nu_{clay}} \frac{D}{\Delta u} (C^w_{ijk+1} - 2C^w_{ijk} + C^w_{ijk-1}) - \frac{dm_{ijk}}{dt} \tag{53}$$

or

$$\frac{dC^w_{ijk}}{dt} = \frac{D}{(\Delta u)^2 \nu_{clay}} (C^w_{ijk+1} - 2C^w_{ijk} + C^w_{ijk-1}) - \frac{n_u}{\omega L \Delta x \Delta y} \frac{dm_{ijk}}{dt}, \quad k = 2, 3, \ldots, n_u - 1 \tag{54}$$

For the innermost slab ($k = n_u$ on either side of the center plane of the lenses), we have

$$\frac{dC^w_{ijnu}}{dt} = \frac{D}{(\Delta u)^2 \nu_{clay}} (-C^w_{ijnu} + C^w_{ijnu-1}) - \frac{n_u}{\omega L \Delta x \Delta y} \frac{dm_{ijnu}}{dt} \tag{55}$$

For the slab adjacent to the advecting gas phase we assume that the aqueous VOC concentration at the air–water interface is given by Henry's

law, so

$$\frac{dC^w_{ij1}}{dt} = \frac{D}{(\Delta u)^2 \nu_{\text{clay}}}[C^w_{ij2} - C^w_{ij1} + 2(C^g_{ij}/K_{\text{H}} - C^w_{ij1})] - \frac{n_u}{\omega L \Delta x \Delta y}\frac{dm_{ij1}}{dt} \tag{56}$$

G. Completion of Gas-Phase VOC Material Balance. The Model

We return to Eq. (20) for the vapor phase advection terms, to which we must adjoin a term corresponding to mass transport of VOC by diffusion from the outermost aqueous slab. This last term is given by

$$\sigma \Delta x \Delta y L \left[\frac{dC^g_{ij}}{dt}\right]_{\text{diff}} = \frac{\omega \Delta x \Delta y L}{l \nu_{\text{clay}}}\frac{D}{(\Delta u/2)}[C^w_{ij1} - C^g_{ij}/K_{\text{H}}] \tag{57}$$

or

$$\left[\frac{dC^g_{ij}}{dt}\right]_{\text{diff}} = \frac{\omega D}{\sigma l \nu_{\text{clay}}(\Delta u/2)}[C^w_{ij1} - C^g_{ij}/K_{\text{H}}] \tag{58}$$

The complete equation is therefore given by

$$\begin{aligned}\frac{dC^g_{ij}}{dt} = {} & \frac{v^{\text{L}}_{ij}}{\sigma \Delta x}[S(v^{\text{L}})C^g_{i-1,j} + S(-v^{\text{L}})C^g_{ij}] \\ & + \frac{v^{\text{R}}_{ij}}{\sigma \Delta x}[-S(-v^{\text{R}})C^g_{i+1,j} - S(v^{\text{R}})C^g_{ij}] \\ & + \frac{v^{\text{B}}_{ij}}{\sigma \Delta y}[S(v^{\text{B}})C^g_{i,j-1} + S(-v^{\text{B}})C^g_{ij}] \\ & + \frac{v^{\text{T}}_{ij}}{\sigma \Delta y}[-S(-v^{\text{T}})C^g_{i,j+1} - S(v^{\text{T}})C^g_{ij}] \\ & + \frac{\omega D}{\sigma l \nu_{\text{clay}}(\Delta u/2)}[C^w_{ij1} - C^g_{ij}/K_{\text{H}}]\end{aligned} \tag{59}$$

Equations (49), (54)–(56), and (59) then constitute the model. The mass of residual VOC is given by

$$M_{\text{tot}} = \sum_{i=1}^{n_x}\sum_{j=1}^{n_y}\left[\Delta V \sigma C^g_{ij} + \sum_{k=1}^{n_u}[m_{ijk} + (\omega \Delta V/n_u)C^w_{ijk}]\right] \tag{60}$$

where $\Delta V = L \Delta x \Delta y$.

The effluent soil gas VOC concentration is most readily calculated from

$$C^g_{\text{eff}} = -\frac{M_{\text{tot}}(t + \Delta t) - M_{\text{tot}}(t)}{q(t)\Delta t} \tag{61}$$

where q is the volumetric gas flow rate.

II. Model for SVE with a Single Vertical Well Screened at the Bottom

Again we assume a homogeneous isotropic porous medium for the calculation of the flow field of the soil gas in the vicinity of the well. See Fig. 5 for the geometry and notation. We shall work in cylindrical coordinates r, z. Symbols not defined in this part are as defined in Part I. As before, we have

$$\nabla^2 P^2 = 0 \tag{1'}$$

with boundary conditions physically identical to those used in the first model,

$$\frac{\partial P^2(r, 0)}{\partial z} = 0 \tag{62}$$

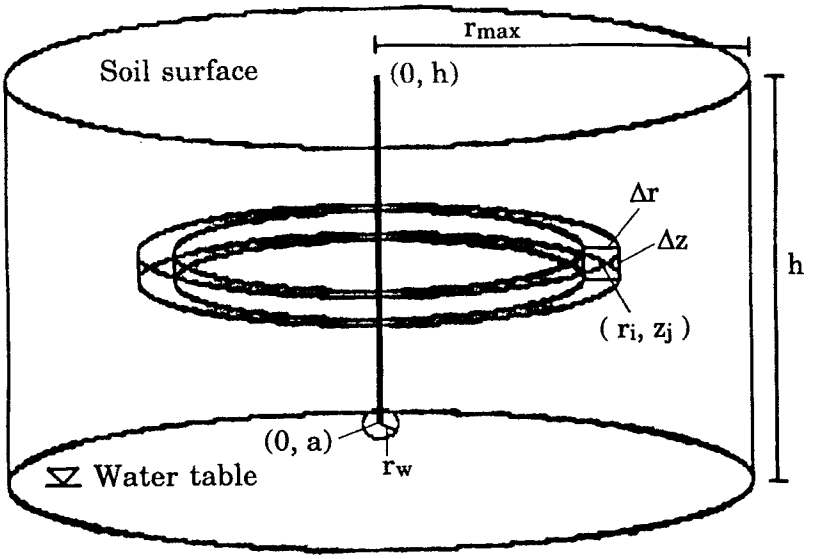

FIG. 5 SVE well, single vertical well screened only near the bottom; geometry and notation.

at the water table, and

$$P^2(r, h) = P_a^2 = 1 \text{ atm}^2 \tag{63}$$

at the soil surface. Define a potential function $W(r, z)$ by

$$W(r, z) + P_a^2 = P^2(r, z) \tag{64}$$

so the problem becomes

$$\nabla^2 W = 0 \tag{65}$$

$$\frac{\partial W(r, 0)}{\partial z} = 0 \tag{66}$$

$$W(r, h) = 0 \tag{67}$$

There must also be a sink at $(0, a)$ to represent the vacuum well.

Again we use the method of images to construct W; it is given by

$$\begin{aligned} W = A \sum_{n=-\infty}^{\infty} \Bigg[& - \frac{1}{\{r^2 + [z - 4nh - a]^2\}^{1/2}} \\ & - \frac{1}{\{r^2 + [z - 4nh + a]^2\}^{1/2}} \\ & + \frac{1}{\{r^2 + [z - (4n - 2)h - a]^2\}^{1/2}} \\ & + \frac{1}{\{r^2 + [z - (4n - 2)h + a]^2\}^{1/2}} \Bigg] \end{aligned} \tag{68}$$

The constant A is evaluated by the requirement that at $(0, a + r_w)$, $P = P_w$, the wellhead pressure. Here r_w is the radius of the well gravel packing. This gives

$$W(0, a + r_w) = P_w^2 - P_a^2 \tag{69}$$

or

$$\begin{aligned} P_w^2 - P_a^2 = A \sum_{n=-\infty}^{\infty} \Bigg[& - \frac{1}{|r_w - 4nh|} - \frac{1}{|2a + r_w - 4nh|} \\ & + \frac{1}{|r_w - (4n - 2)h|} + \frac{1}{|2a + r_w - (4n - 2)h|} \Bigg] \\ = AS & \end{aligned} \tag{70}$$

and so

$$A = (P_w^2 - P_a^2)/S \tag{71}$$

where S is the sum appearing on the right-hand side of Eq. (70).

The molar flow rate to the well is given by

$$Q = -\int_0^{2\pi}\int_0^{\pi} c v_\rho \rho^2 \sin\theta \, d\theta \, d\phi \tag{72}$$

where

$$v_\rho = -K_D \nabla_\rho P \tag{73}$$

and $c = P/RT$. This can be rearranged to give

$$QRT = q = \int_0^{2\pi}\int_0^{\pi} K_D(1/2)[\nabla_\rho P^2]\rho^2 \sin\theta \, d\theta \, d\phi \tag{74}$$

or

$$q = \int_0^{2\pi}\int_0^{\pi} (1/2)K_D(\nabla_\rho W)\rho^2 \sin\theta \, d\theta \, d\phi \tag{75}$$

When the integration is carried out over the surface of a small sphere containing the screened section of the well, the only term from W which contributes is the first of the four terms, and that only when $n = 0$. In the integral we can therefore write

$$W = -A/\rho \tag{76}$$

so

$$\nabla_\rho W = A/\rho^2 \tag{77}$$

and q is given by

$$q = \frac{K_D A}{2\rho^2}\int_0^{2\pi}\int_0^{\pi} \rho^2 \sin\theta \, d\theta \, d\phi = 2\pi A K_D \tag{78}$$

Then

$$A = q/(2\pi K_D) \tag{79}$$

Setting this result equal to the right-hand side of Eq. (71) and solving for K_D then gives

$$K_D = \frac{qS}{2\pi(P_w^2 - P_a^2)} \tag{80}$$

The superficial velocity of the gas is given, as before, by Eq. (19), except that here the components of ∇W are $\partial W/\partial r$ and $\partial W/\partial z$, and the velocity components are v_r and v_z.

A. Volume Elements and Surfaces of Volume Elements. Advective Mass Balance

See Fig. 5. The volume of the annular volume element is given by

$$\Delta V_{ij} = (2i - 1)\pi(\Delta r)^2 \Delta z \tag{81}$$

The surfaces of this volume element are as follows:

$$\text{Inner} \qquad S_{ij}^{\mathrm{I}} = 2(i - 1)\pi \Delta r \Delta z \tag{82}$$

$$\text{Outer} \qquad S_{ij}^{0} = 2i\pi \Delta r \Delta z \tag{83}$$

$$\text{Top and Bottom} \qquad S_{ij}^{\mathrm{T}} = S_{ij}^{\mathrm{B}} = (2i - 1)\pi(\Delta r)^2 \tag{84}$$

The advective mass balance for VOC in this volume element is then

$$\begin{aligned} \Delta V_{ij}\left[\frac{dC_{ij}^{g}}{dt}\right]_{\mathrm{adv}} &= S_{ij}^{\mathrm{I}} v_{ij}^{\mathrm{I}}[S(v^{\mathrm{I}})C_{i-1,j}^{g} + S(-v^{\mathrm{I}})C_{ij}^{g}] \\ &+ S_{ij}^{0} v_{ij}^{0}[-S(-v^{0})C_{i+1,j}^{g} - S(v^{0})C_{ij}^{g}] \\ &+ S_{ij}^{\mathrm{B}} v_{ij}^{\mathrm{B}}[S(v^{\mathrm{B}})C_{i,j-1}^{g} + S(-v^{\mathrm{B}})C_{ij}^{g}] \\ &+ S_{ij}^{\mathrm{T}} v_{ij}^{\mathrm{T}}[-S(-v^{\mathrm{T}})C_{i,j+1}^{g} - S(v^{\mathrm{T}})C_{ij}^{g}] \end{aligned} \tag{85}$$

where

$$v_{ij}^{\mathrm{I}} = v_r[(i - 1)\Delta r, (j - 1/2)\Delta z] \tag{86}$$

$$v_{ij}^{0} = v_r[i\Delta r, (j - 1/2)\Delta z] \tag{87}$$

$$v_{ij}^{\mathrm{B}} = v_z[(i - 1/2)\Delta r, (j - 1)\Delta z] \tag{88}$$

$$v_{ij}^{\mathrm{T}} = v_z[(i - 1/2)\Delta r, j\Delta z] \tag{89}$$

B. Initial Distribution of VOC among Phases

This is handled exactly as in the earlier model, Part I.D of this section.

C. Rate of Change of NAPL Mass

Analysis essentially identical to that resulting in Eq. (49) leads to

$$\frac{dm_{ijk}}{dt} = -\frac{3\Delta V_{ij} C_0^N D(C_{\mathrm{sat}} - C_{ijk}^{w})(m_{ijk}/m_{ij}^{0})^{1/3}}{n_u a_0^2 \rho_{\mathrm{voc}}[1 - (a_0/b)(m_{ijk}/m_{ij}^{0})^{1/3}]} \tag{90}$$

Here

$$m_{ij}^{0} = C_0^N \Delta V_{ij}/n_u \tag{91}$$

the initial mass of NAPL in the kth slab of the volume element ΔV_{ij}.

D. Change in Aqueous VOC Concentration

Analysis similar to that of Part I.F leads to

$$\frac{dC^w_{ijk}}{dt} = \frac{D}{(\Delta u)^2 \nu_{\text{clay}}}(C^w_{ij,k+1} - 2C^w_{ijk} + C^w_{ij,k-1}) - \frac{n_u}{\omega \Delta V_{ij}}\frac{dm_{ijk}}{dt}, \quad k = 2, 3, \ldots, n_u - 1 \tag{92}$$

For the innermost slab,

$$\frac{dC^w_{ijnu}}{dt} = \frac{D}{(\Delta u)^2 \nu_{\text{clay}}}(-C^w_{ijnu} + C^w_{ij,nu-1}) - \frac{n_u}{\omega \Delta V_{ij}}\frac{dm_{ijnu}}{dt} \tag{93}$$

For the slab adjacent to the advecting gas phase,

$$\frac{dC^w_{ij1}}{dt} = \frac{D}{(\Delta j)^2 \nu_{\text{clay}}}[C^w_{ij2} - C^w_{ij1} + 2(C^g_{ij}/K_{\text{H}} - C^w_{ij1})] - \frac{n_u}{\omega \Delta V_{ij}}\frac{dm_{ij1}}{dt} \tag{94}$$

E. Completion of the Gas-Phase Material Balance. The Model

We obtain the advection terms in the mass balance for gaseous VOC from Eq. (85). The term modeling diffusion from the first aqueous layer is

$$\sigma \Delta V_{ij}\left[\frac{dC^g_{ij}}{dt}\right]_{\text{diff}} = \frac{\omega \Delta V_{ij}}{l\nu_{\text{clay}}}\frac{D}{(\Delta u/2)}[C^w_{ij1} - C^g_{ij}/K_{\text{H}}] \tag{95}$$

or

$$\left[\frac{dC^g_{ij}}{dt}\right]_{\text{diff}} = \frac{\omega D}{\sigma l \nu_{\text{clay}}(\Delta u/2)}[C^w_{ij1} - C^g_{ij}/K_{\text{H}}] \tag{96}$$

The complete equation is therefore given by

$$\begin{aligned}\frac{dC^g_{ij}}{dt} = {} & \frac{S^{\text{I}}_{ij} v^{\text{I}}_{ij}}{\sigma \Delta V_{ij}}[S(v^{\text{I}})C^g_{i-1,j} + S(-v^{\text{I}})C^g_{ij}] \\ & + \frac{S^{\text{O}}_{ij} v^{\text{O}}_{ij}}{\sigma \Delta V_{ij}}[-S(-v^{\text{O}})C^g_{i+1,j} - S(v^{\text{O}})C^g_{ij}] \\ & + \frac{S^{\text{B}}_{ij} v^{\text{B}}_{ij}}{\sigma \Delta V_{ij}}[S(v^{\text{B}})C^g_{i,j-1} + S(-v^{\text{B}})C^g_{ij}]\end{aligned} \tag{97}$$

$$+ \frac{S_{ij}^{T} v_{ij}^{T}}{\sigma \Delta V_{ij}} [-S(-v^{T}) C_{i,j+1}^{g} - S(v^{T}) C_{ij}^{g}]$$

$$+ \frac{D}{\sigma l v_{clay}(\Delta u/2)} (C_{ij1}^{w} - C_{ij}^{g}/K_{H})$$

Equations (90), (92)–(94), and (97) then constitute the model. The mass of residual VOC at any time during the course of a simulation is given by

$$M_{tot} = \sum_{i=1}^{n_r} \sum_{j=1}^{n_z} \left\{ \Delta V_{ij} \sigma C_{ij}^{g} + \sum_{k=1}^{n_u} \left[m_{ijk} + \frac{\omega \Delta V_{ij}}{n_u} C_{ijk}^{w} \right] \right\} \tag{98}$$

The effluent soil gas concentration is given by Eq. (61), repeated here for convenience.

$$C_{eff}^{g} = - \frac{M_{tot}(t + \Delta t) - M_{tot}(t)}{q(t) \Delta t} \tag{61'}$$

An alternative approach to C_{eff}^{g} is to define it as follows. Let V_{1J} be the volume element containing the well. Then

$$C_{eff}^{g} = \frac{S_{1J}^{T} \mid v_{1J}^{T} \mid C_{1,J+1}^{g} + S_{1J}^{O} \mid v_{1J}^{O} \mid C_{2J}^{g} + S_{1J}^{B} \mid v_{1J}^{B} \mid C_{1,J-1}^{g}}{S_{1J}^{T} \mid v_{1J}^{T} \mid + S_{1J}^{O} \mid v_{1J}^{O} \mid + S_{1J}^{B} \mid v_{1J}^{B} \mid} \tag{99}$$

RESULTS

These models were implemented in TurboBASIC on an AlphaSystem 486-DX microcomputer running at 50 MHz. Typical runs with the model for SVE with a horizontal slotted pipe required about 3 minutes; runs with the single vertical well SVE model required about 8 minutes since these required a substantially smaller value of Δt in the numerical integration to avoid unstable behavior due to the high gas velocities in the immediate vicinity of the well. Default parameters for the horizontal slotted pipe runs are given in Table 1; parameters for the vertical well runs are given in Table 2. Departures from these values are indicated in the text and in the captions to the figures. The plots are of two types: figures labeled "a" show plots of $M'_{tot} = M_{tot}(t)/M_{tot}(0)$ versus time, and figures labeled "b" display plots of $C_{eff}^{g\prime} = C_{eff}^{g}(t)/(K_H C_{sat})$, which is the fraction of VOC saturation of the effluent gas. Plots of the first type give information about how much VOC is left—how the cleanup is progressing. Plots of the second type are plots of a quantity which can readily be measured during the course of the cleanup and which has often been used to attempt to follow the course of the cleanup.

TABLE 1
Default Parameters Used with the Horizontal Slotted Pipe Model

Width of domain to be stripped	10 m
Depth of domain to be stripped	5 m
Breadth of domain to be stripped (length of pipe)	10 m
Depth of well	4.5 m
Volumetric gas flow rate of well	25 SCFM (0.0118 m^3/s)
Wellhead pressure	0.9 atm
Diameter of well gravel packing	30 cm
Identity of VOC	Trichloroethylene, TCE
Aqueous solubility of VOC	1100 mg/L
Henry's constant of VOC (dimensionless)	0.2821
Effective diffusion constant of VOC (diffusivity × tortuosity/ν_{clay})	2×10^{-10} m^2/s
Density of VOC	1.46 g/cm^3
Soil density	1.7 g/cm^3
Soil air-filled porosity	0.2
Soil water-filled porosity	0.2
Mean half-thickness l of porous clay lenses	1.0 cm
Initial NAPL droplet diameter	0.1 cm
n_x	5
n_y	5
n_u	5
Total VOC concentration in the soil	2000 mg/kg
Δt	900 seconds
Duration of simulated run	100 days
Calculated Darcy's constant	0.01106 $m^2/atm \cdot s$

Figures 6(a) and 6(b) show the effect of the half-thickness l of the clay lenses on cleanups with a horizontal slotted pipe SVE well: $l = 0.5, 0.75, 1.0, 1.25$, and 1.5 cm. The time required for cleanup increases drastically with increasing values of l, although the same gas flow rates and same initial total VOC masses are used throughout. The reduced concentration plots in Fig. 6(b) indicate the difficulty of using effluent soil gas VOC concentrations alone as a guide to the progress of the cleanup. Initial extremely rapid rates of removal (lasting less than a day) are followed by rapid decreases in effluent soil gas VOC levels, which then gradually decrease, with some fits and starts, to zero as the cleanup proceeds. About the only firm conclusion one can draw from the concentration plots is that when cleanup is complete, the effluent soil gas VOC concentration is zero, which, while true, is not very helpful.

The effect of air flow rate on cleanup for horizontal slotted pipe wells is shown in Figs. 7(a) and 7(b). Air flow rates are 50, 25, 12.5, and 6.25 SCFM (0.02360, 0.01180, 0.00590, and 0.00295 m^3/s. The half-thickness of the clay lenses is 1.0 cm. It is evident from Fig. 7(a) that there is virtually nothing to be gained in terms of increased cleanup time by operating the well at flow rates above 12.5 SCFM—at these flow rates the process is completely diffusion-controlled. And it is obvious from Fig. 7(b) that one is going to have to treat much larger volumes of off-gas containing much lower concentrations of VOCs at the higher flow rates, which is costly.

The effect of NAPL droplet size on VOC removal rate is shown in Figs. 8(a) and 8(b). Droplet diameters are 0.01, 0.05, 0.1, 0.2, and 0.3 cm, and the well configuration is that of a horizontal slotted pipe. The half-thickness of the clay lenses is held constant at 1 cm. As the droplet size increases, the total NAPL/water interface of the droplets decreases, decreasing the rate at which the NAPL dissolves. In Runs 4 and 5 (droplet diameters of 0.2

TABLE 2
Default Parameters Used with the Vertical Well Model

Radius of domain to be stripped	5 m
Depth of domain to be stripped	5 m
Depth of well	4.5 m
Volumetric gas flow rate of well	25 SCFM ($0.0118\ m^3/s$)
Wellhead pressure	0.9 atm
Diameter of well gravel packing	30 cm
Identity of VOC	Trichloroethylene, TCE
Aqueous solubility of VOC	1100 mg/L
Henry's constant of VOC (dimensionless)	0.2821
Effective diffusion constant of VOC (diffusivity × tortuosity/ν_{clay})	$2 \times 10^{-10}\ m^2/s$
Density of VOC	$1.46\ g/cm^3$
Soil density	$1.7\ g/cm^3$
Soil air-filled porosity	0.2
Soil water-filled porosity	0.2
Mean half-thickness l of porous clay lenses	1.0 cm
Initial NAPL droplet diameter	0.1 cm
n_r	5
n_z	5
n_u	5
Total VOC concentration in the soil	2000 mg/kg
Δt	150 seconds
Duration of simulated run	100 days
Calculated Darcy's constant	$0.04904\ m^2/atm \cdot s$

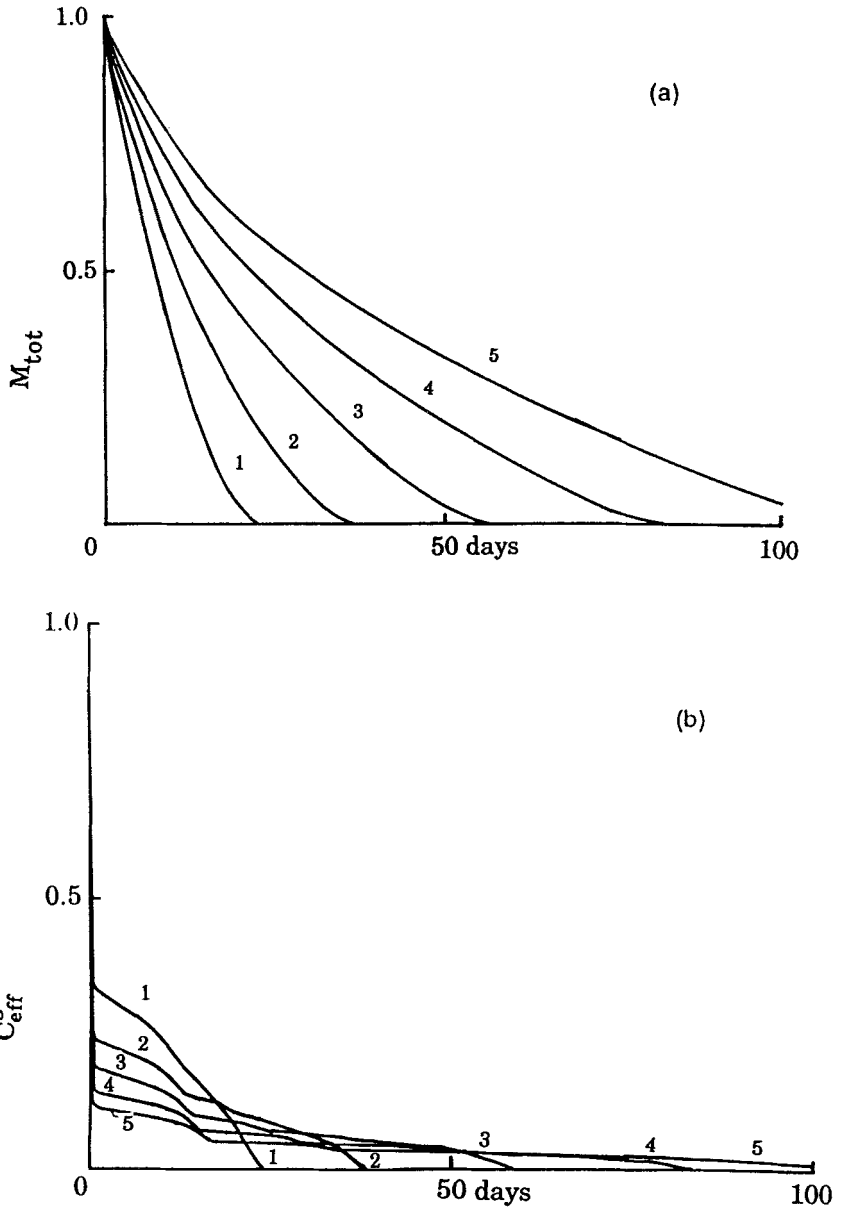

FIG. 6 Plots of reduced mass of residual VOC (a) and reduced effluent soil gas VOC concentration (b); effect of half-thickness l of clay lenses. l = 0.5, 0.75, 1.0, 1.25, and 1.5 cm, 1 through 5. Other parameters as in Table 1. Configuration is a buried horizontal slotted pipe.

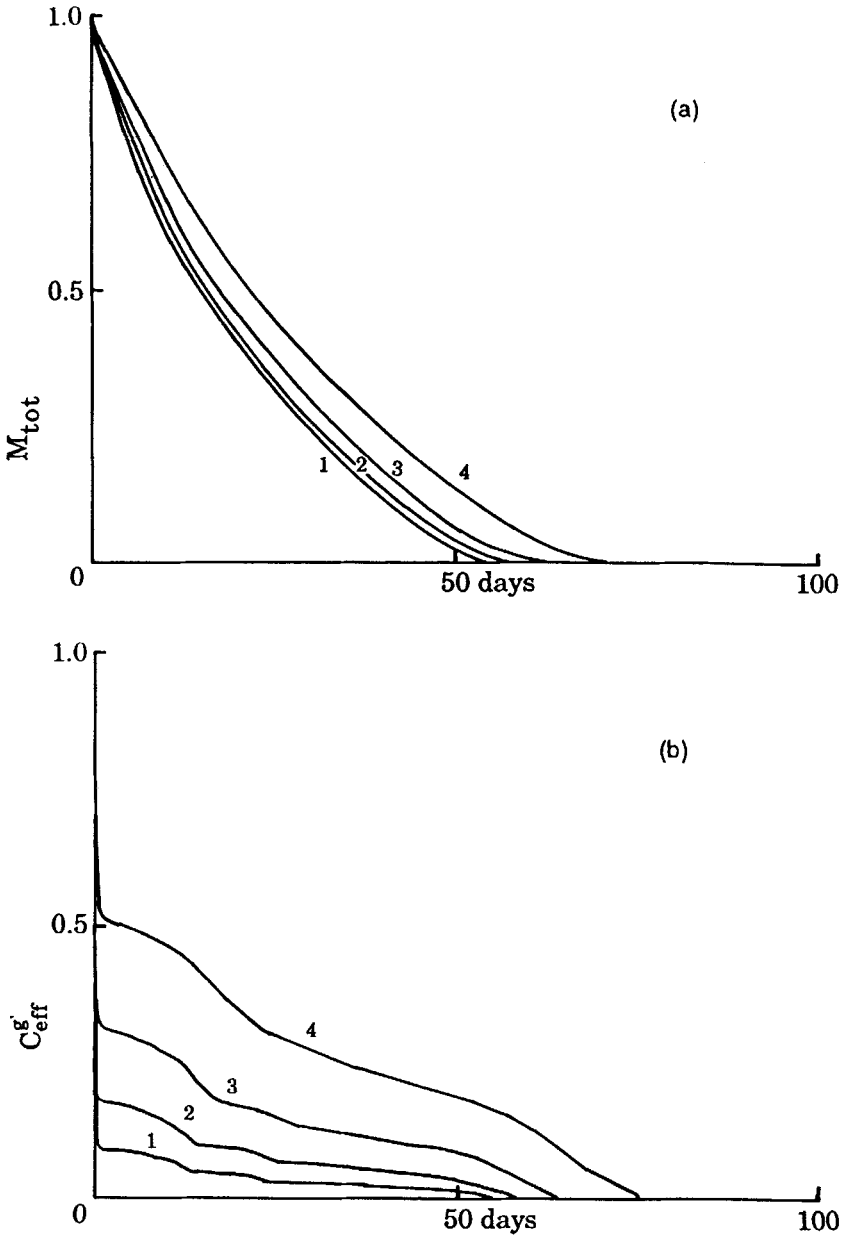

FIG. 7 Plots of reduced mass of residual VOC (a) and reduced effluent soil gas VOC concentration (b); effect of well gas flow rate. q = 50, 25, 12.5, and 6.25 SCFM, 1 through 4. Other parameters as in Table 1. Configuration is a buried horizontal slotted pipe.

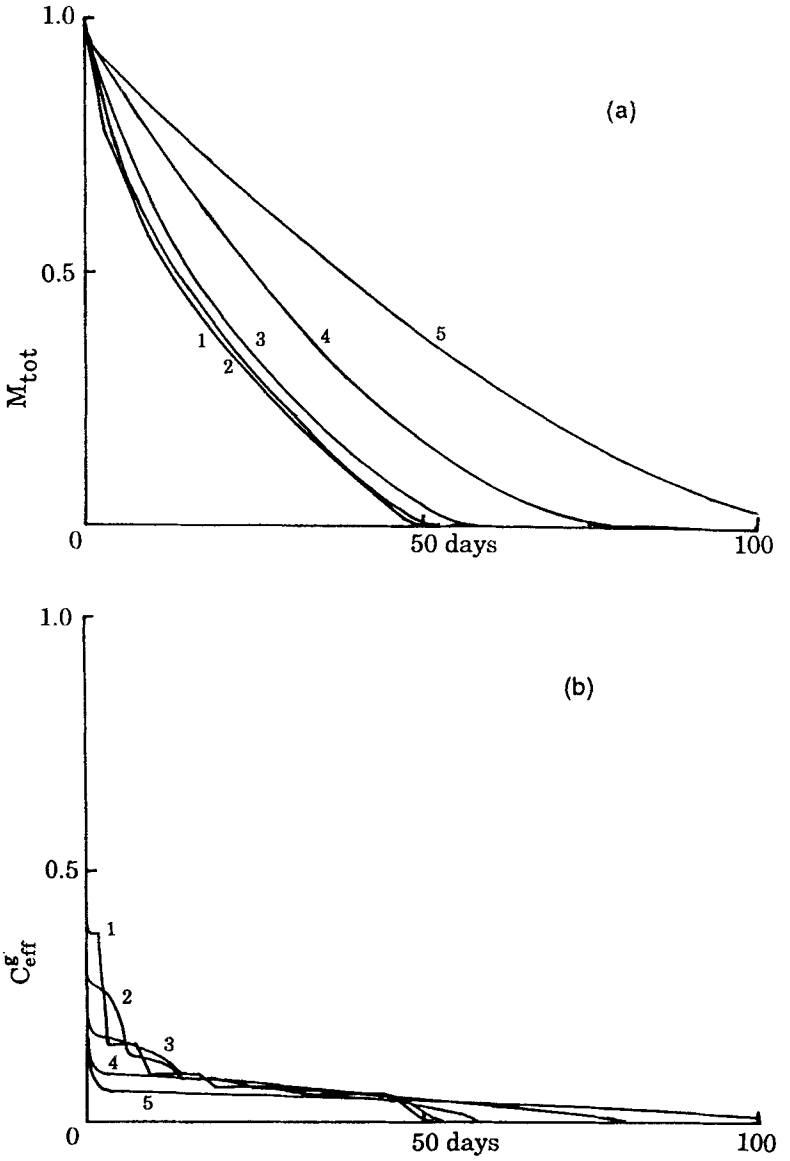

FIG. 8 Plots of reduced mass of residual VOC (a) and reduced effluent soil gas VOC concentration (b); effect of initial diameter of NAPL droplets. a_0 = 0.01, 0.05, 0.10, 0.20, and 0.30 cm, 1 through 5. Other parameters as in Table 1. Configuration is a buried horizontal slotted pipe.

and 0.3 cm), the rate of solution of the droplets is becoming the controlling factor rather than the diffusion of dissolved VOC through the aqueous phase in the clay lenses. The sharp structure of some of the effluent soil gas VOC concentration plots is a mathematical artifact which varies depending on the number of slabs used to represent the clay lenses. Increasing the number of slabs smooths these out but adds drastically to computer time requirements.

Figures 9(a) and 9(b) show the effects of varying the initial VOC concentration in the soil. The horizontal slotted pipe configuration is used. Initial concentrations are 250, 500, 1000, 1500, 2000, 2500, and 3000 mg/kg. Cleanup times are seen to be roughly proportional to the initial concentration of VOC, at least at the higher concentrations. Even at the highest concentrations one does not find effluent soil gas VOC concentrations approaching anywhere near the saturation value after the first few hours of the run, indicating that mass transport kinetics are limiting even under these conditions. In interpreting Fig. 9(a), recall that the ordinate is $M_{tot}(t)/M_{tot}(0)$, so all the curves pass through the point (0, 1), even though the initial masses for these runs are different.

In Figs. 10(a) and 10(b) we compare a matched pair of runs made with the horizontal slotted pipe model (H) and the vertical well model (V). The default parameters given in Tables 1 and 2 were used for these two runs. The cleanup time of the vertical well is some 39.8% larger than that of the horizontal slotted pipe well, despite the fact that the horizontal slotted pipe well must remove 1632 kg of VOC while the vertical well is removing only 1324 kg. Gas flow rates are 25 SCFM in both cases. We conclude that the horizontal slotted pipe configuration is intrinsically more efficient than the single vertical well configuration. This is a point which we have noticed previously with some of our other models. Evidently significant savings in operating costs could result from use of the horizontal slotted pipe configuration, provided that the wells were sufficiently shallow that installation could be readily carried out.

The effects of initial NAPL droplet diameter on SVE by means of a single vertical well are shown in Figs. 11(a) and 11(b). Initial droplet diameters are 0.025, 0.05, 0.075, 0.10, 0.15, and 0.20 cm. As with the other model, we find that increased droplet diameter very markedly reduces the rate of cleanup due to the decrease in total NAPL–water interface.

Figures 12(a) and 12(b) exhibit the effect of varying the half-thickness of the clay lenses. Values of l are 0.5, 1.0, and 1.5 cm. As before, increased thicknesses of the lenses results in greatly decreased removal rates. The low effluent soil gas VOC concentrations seen in Fig. 12(b) indicate that all of these runs are in the diffusion-controlled regime. Note the rather long plateaus in the effluent soil gas VOC concentration plots and the

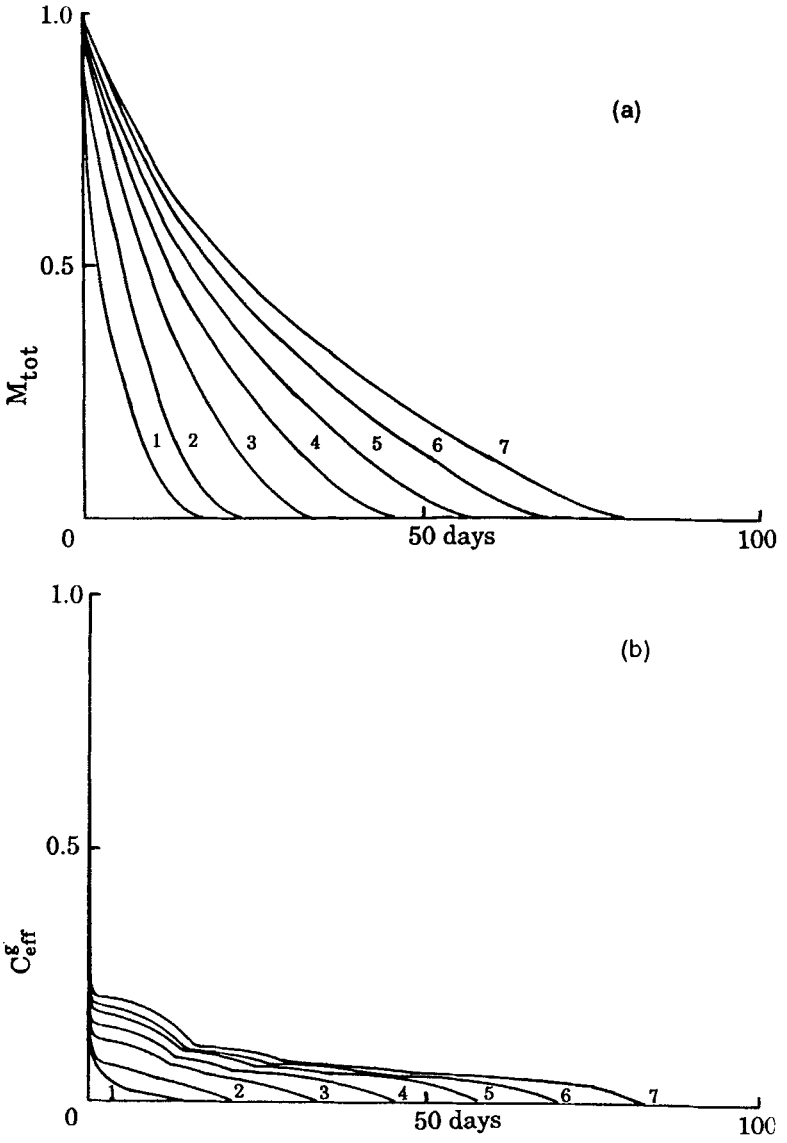

FIG. 9 Plots of reduced mass of residual VOC (a) and reduced effluent soil gas VOC concentration (b); effect of initial VOC concentration. C_{tot0} = 250, 500, 1000, 1500, 2000, 2500, and 3000 mg/kg, 1 through 7. Other parameters as in Table 1. Configuration is a buried horizontal slotted pipe.

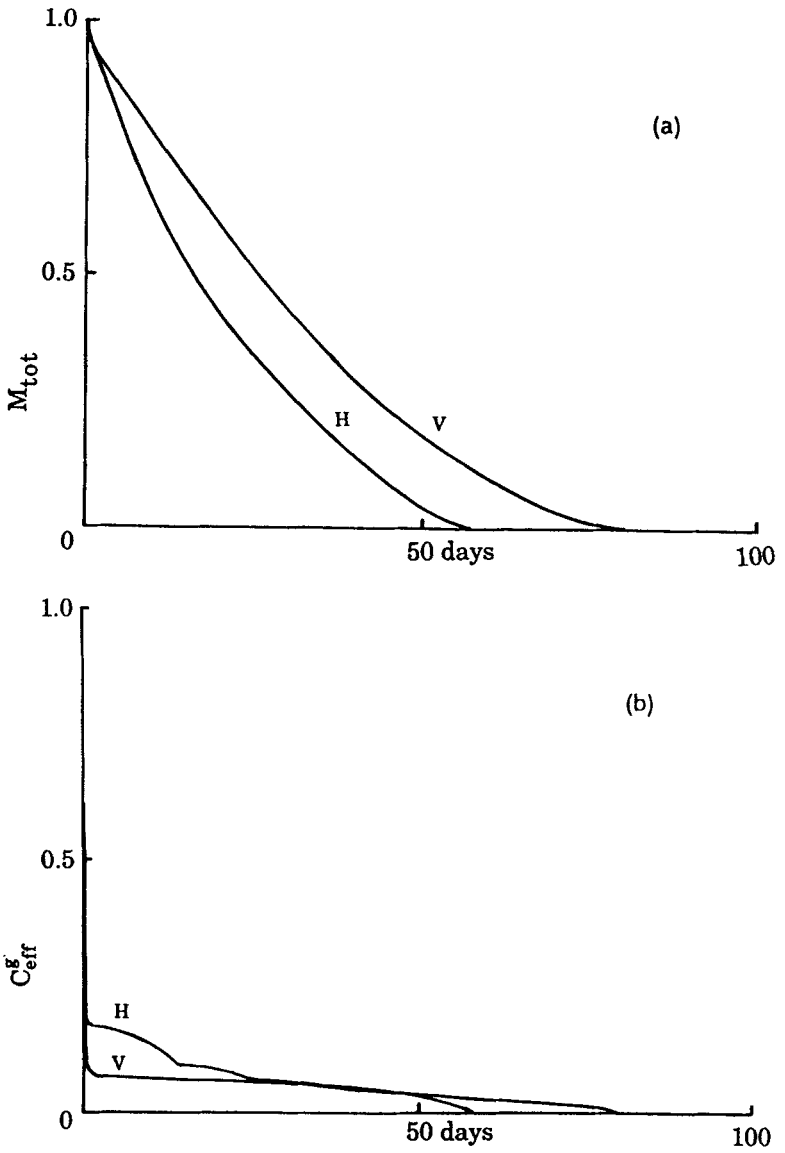

FIG. 10 Plots of reduced mass of residual VOC (a) and reduced effluent soil gas VOC concentration (b); effect of well configuration. H: Horizontal slotted pipe configuration, parameters as in Table 1. V: Vertical well configuration, parameters as in Table 2.

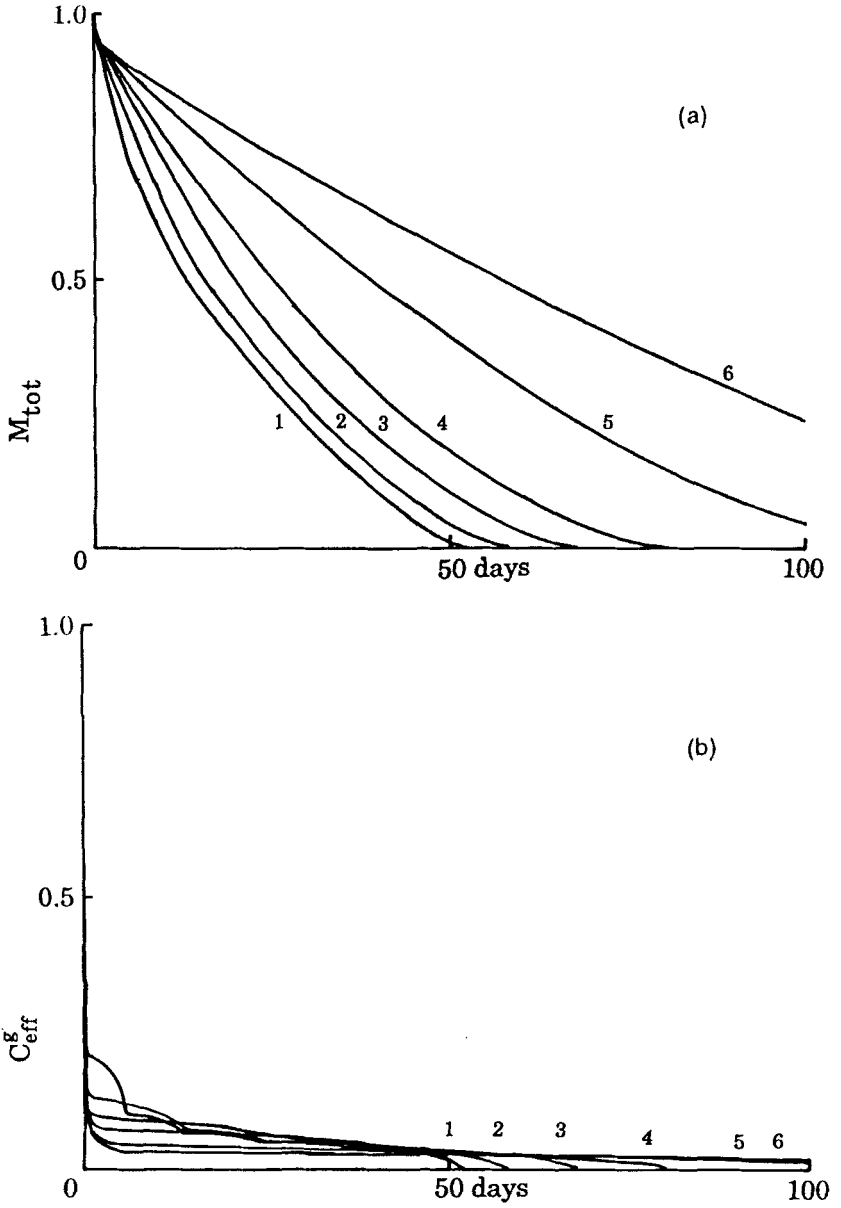

FIG. 11 Plots of reduced mass of residual VOC (a) and reduced effluent soil gas VOC concentration (b); effect of initial NAPL droplet diameter size. a_0 = 0.025, 0.050, 0.075, 0.10, 0.15, and 0.20 cm, 1 through 6. Other parameters as in Table 2. Configuration is a single vertical well screened only at the bottom.

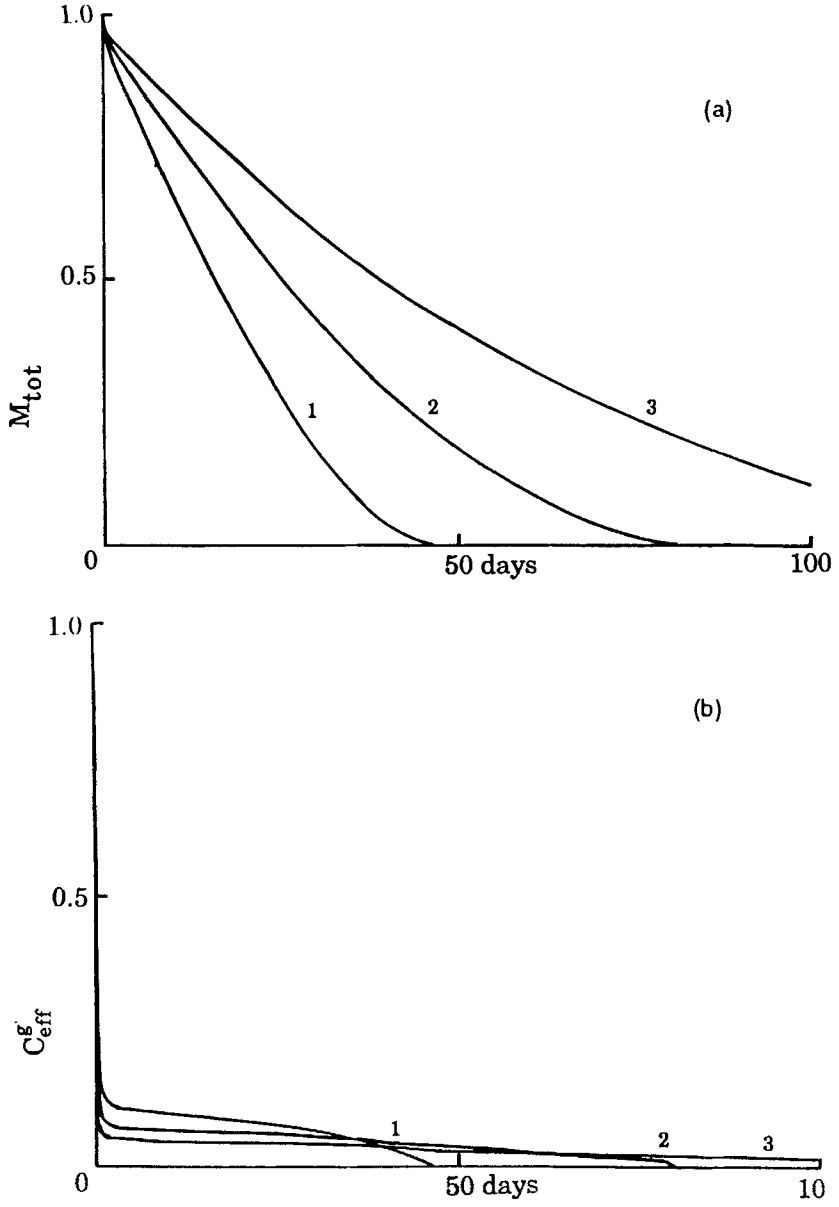

FIG. 12 Plots of reduced mass of residual VOC (a) and reduced effluent soil gas VOC concentration (b); effect of half-thickness l of clay lenses. l = 0.5, 1.0, and 1.5 cm, 1 through 3. Other parameters as in Table 2. Configuration is a single vertical well screened at the bottom.

relatively abrupt decreases to zero at the end of the cleanup, with no prior indication that cleanup is nearly complete.

CONCLUSIONS

Two models for the operation of SVE wells (horizontal slotted pipe and single vertical well configurations) have been developed which take the solution rate of NAPL and the diffusion of VOC through water-saturated clay layers into account in a rather realistic way. Depending on the parameters selected, either solution rate of NAPL or diffusion of dissolved VOC, or both, can be rate-limiting. The shapes of the effluent soil gas VOC concentration curves are such as to discourage interpretation of these alone in terms of the degree of progress of the cleanup. The wastefulness of excessively high pumping speeds for systems which are controlled by solution or diffusion bottlenecks is demonstrated. Data for use in the models should be readily obtainable from well log information. The results also indicate that it will not be possible to develop methods for interpreting data from relatively short-term field pilot studies (of a few days' duration, involving removal of 5–25% of the VOC in the domain of influence of the well) to yield information about the time which will be required to achieve virtually 100% cleanup of the site.

ACKNOWLEDGMENTS

D.J.W. is greatly indebted to the University of Málaga for its hospitality and the use of its facilities, to Dr. J. J. Rodríguez-Jimenez for making his visit to Málaga possible and for helpful discussions of the project, to Vanderbilt University for financial support during his leave, and to the Spanish Government (DGICYT) for a fellowship in support of this work.

REFERENCES

1. T. A. Pedersen and J. T. Curtis, *Soil Vapor Extraction Technology Reference Handbook*, Risk Reduction Engineering Laboratory, U.S. EPA Report EPA/540/2-91/003, 1991. Reprinted as *Soil Vapor Extraction Technology* (Pollution Technology Review 204), (T. A. Pedersen and J. T. Curtis, Eds.), Noyes Publications, Park Ridge, New Jersey, 1991.
2. J. P. Stumbar and J. Rawe, *Guide for Conducting Treatability Studies under CERCLA: Soil Vapor Extraction Interim Guidance*, U.S. EPA Report EPA/540/2-91/019A, 1991.
3. W. J. Lyman and D. C. Noonan, "Assessing UST Corrective Action Technologies: Site Assessment and Selection of Unsaturated Zone Treatment Technologies," in *Cleanup of Petroleum Contaminated Soils at Underground Storage Tanks* (by W. J. Lyman, D. C. Noonan and P. J. Reidy), Noyes Data Corp., Park Ridge, New Jersey, 1990.

4. P. J. Reidy, W. J. Lyman, and D. C. Noonan, "Saturated Zone Corrective Action Technologies," in *Cleanup of Petroleum Contaminated Soils at Underground Storage Tanks* (by W. J. Lyman, D. C. Noonan and P. J. Reidy), Noyes Data Corp., Park Ridge, New Jersey, 1990.
5. *Proceedings, Symposium on Soil Venting, April 29–May 1, 1991, Houston, TX*, D. DiGiulio, project officer, U.S. EPA Report EPA/600/R-92/174.
6. N. J. Hutzler, B. E. Murphy, and J. S. Gierke, "State of Technology Review: Soil Vapor Extraction Systems," *J. Hazard. Mater., 26*(2), 225 (1991).
7. N. J. Hutzler, B. E. Murphy, and J. S. Gierke, *Review of Soil Vapor Extraction System Technology*, Presented at the Soil Vapor Extraction Technology Workshop, U.S. EPA Risk Reduction Engineering Laboratory (RREL), June 28–29, 1989, Edison, New Jersey. Reprinted in *Soil Vapor Extraction Technology* (Pollution Technology Review 204), (T. A. Pedersen and J. T. Curtis, Eds.), Noyes Publications, Park Ridge, New Jersey, 1991, p. 136.
8. D. J. Wilson and A. N. Clarke, "Soil Vapor Extraction," in *Hazardous Waste Site Soil Remediation: Theory and Application of Innovative Technologies* (D. J. Wilson and A. N. Clarke, Eds.), Dekker, New York, 1993, p. 171.
9. A. L. Baehr, G. E. Hoag, and M. C. Marley, "Removing Volatile Contaminants from the Unsaturated Zone by Inducing Advective Air-Phase Transport," *J. Contam. Hydrol., 4*, 1 (1989).
10. G. E. Hoag, *Soil Vapor Extraction Research Developments*, Presented at the Soil Vapor Extraction Technology Workshop, U.S. EPA RREL, June 28–29, 1989, Edison, New Jersey. Reprinted in *Soil Vapor Extraction Technology* (Pollution Technology Review 204), (T. A. Pedersen and J. T. Curtis, Eds.), Noyes Publications, Park Ridge, New Jersey, 1991, p. 286.
11. G. E. Hoag, C. J. Bruell, and M. C. Marley, *Study of the Mechanisms Controlling Gasoline Hydrocarbon Partitioning and Transport in Ground Water Systems*, USGS Report G832-06, available from NTIS as PB85-242907/AS, 1984.
12. G. E. Hoag, M. C. Marley, B. L. Cliff, and P. Nangeroni, "Soil Vapor Extraction Research Developments," in *Hydrocarbon Contaminated Soils and Ground Water: Analysis, Fate, Environmental and Public Health Effects, and Remediation*, Lewis Publishers, Chelsea, Michigan, 1991, p. 187.
13. M. C. Marley, "Development and Application of a Three-Dimensional Air Flow Model in the Design of a Vapor Extraction System," in *Proceedings, Symposium on Soil Venting, April 29–May 1, 1991, Houston, TX*, D. DiGiulio, project officer, U.S. EPA Report EPA/600/R-92/174, 1992, p. 125.
14. M. C. Marley, P. E. Nangeroni, B. L. Cliff, and J. D. Polonsky, "Air Flow Modeling for In Situ Evaluation of Soil Properties and Engineered Vapor Extraction System Design," in *Proceedings, 4th National Outdoor Action Conference on Aquifer Restoration, Ground Water Monitoring and Geophysical Methods, May 14–17, 1992, Las Vegas, NV*, p. 651.
15. M. C. Marley, S. D. Richter, B. L. Cliff, and P. E. Nangeroni, *Design of Soil Vapor Extraction Systems—A Scientific Approach*, Presented at the Soil Vapor Extraction Technology Workshop, U.S. EPA RREL, June 28–29, 1989, Edison, New Jersey. Reprinted in *Soil Vapor Extraction Technology* (Pollution Technology Review 204), (T. A. Pedersen and J. T. Curtis, Eds.), Noyes Publications, Park Ridge, New Jersey.
16. P. C. Johnson, M. W. Kemblowski, and J. D. Colthart, *Practical Screening Models for Soil Venting Applications*, Presented at the Workshop on Soil Vacuum Extraction, April 27–28, 1989, RSKERL, Ada, OK.
17. P. C. Johnson, M. W. Kemblowski, and J. D. Colthart, "Quantitative Analysis for the

Cleanup of Hydrocarbon-Contaminated Soils by In Situ Soil Venting," *Ground Water*, *28*, 413 (1990).

18. P. C. Johnson, M. W. Kemblowski, J. D. Colthart, D. L. Byers, and C. C. Stanley, *A Practical Approach to the Design, Operation, and Monitoring of In-Situ Soil Venting Systems*, Presented at the Soil Vapor Extraction Technology Workshop, June 28–29, 1989, U.S. EPA RREL, Edison, New Jersey. Reprinted in *Soil Vapor Extraction Technology* (Pollution Technology Review 204), (T. A. Pedersen and J. T. Curtis, Eds.), Noyes Publications, Park Ridge, New Jersey, 1991, p. 195.
19. P. C. Johnson, C. C. Stanley, M. W. Kemblowski, D. L. Byers, and J. D. Colthart, "Practical Approach to the Design, Operation and Monitoring of In Situ Soil Venting Systems," *Ground Water Monit. Rev.*, *10*, 159 (1990).
20. M. W. Kemblowski and S. Chowdery, "Soil Venting Design: Models and Decision Analysis," in *Proceedings, Symposium on Soil Venting, April 29–May 1, 1991, Houston, TX*, D. DiGiulio, project officer, U.S. EPA Report EPA/600/R-92/174, 1992, p. 73.
21. J. S. Cho, *Forced Air Ventilation for Remediation of Unsaturated Soils Contaminated by VOC*, U.S. EPA Report EPA/600/2-91/016, July 1991.
22. J. C. Walton, R. G. Baca, J. B. Sisson, and T. R. Wood, "Application of Soil Venting at a Large Scale: A Data and Modeling Analysis," in *Proceedings, 4th National Outdoor Action Conference on Aquifer Restoration, Ground Water Monitoring and Geophysical Methods, May 14–17, Las Vegas, NV*, 1990, p. 559.
23. J. C. Walton, R. G. Baca, J. B. Sisson, A. J. Sondrup, and S. O. Magnusen, "Application of Computer Simulation Models to the Design of a Large-Scale Soil Venting System and Bioremediation," in *Proceedings, Symposium on Soil Venting, April 29–May 1, 1991, Houston, TX*, D. DiGiulio, project officer, U.S. EPA Report EPA/600/R-92/174, 1992, p. 91.
24. D. J. Wilson, A. N. Clarke, and J. H. Clarke, "Soil Cleanup by In Situ Aeration. I. Mathematical Modeling," *Sep. Sci. Technol.*, *23*, 991 (1988).
25. K. Gannon, D. J. Wilson, A. N. Clarke, R. D. Mutch, and J. H. Clarke, "Soil Cleanup by In Situ Aeration. II. Effects of Impermeable Caps, Soil Permeability, and Evaporative Cooling," *Ibid.*, *24*, 831 (1989).
26. A. N. Clarke, M. M. Megehee, and D. J. Wilson, "Soil Cleanup by In Situ Aeration. XII. Effect of Departures from Darcy's Law on Soil Vapor Extraction," *Ibid.*, *28*, 1671 (1993).
27. W. R. Roy and R. A. Griffin, *In-Situ Extraction of Organic Vapors from Unsaturated Porous Media*, Environmental Institute for Waste Management Studies, University of Alabama, Tuscaloosa, Open File Report 24, 1989.
28. M. C. Marley and G. E. Hoag, *Induced Venting for the Recovery/Restoration of Gasoline Hydrocarbons in the Vadose Zone*, Presented at the NWWA/API Conference on Petroleum Hydrocarbons and Organic Chemicals in Groundwater, Houston, Texas, November 5–7, 1984.
29. D. C. DiGiulio, J. S. Cho, R. R. Dupont, and M. W. Kemblowski, "Conducting Field Tests for Evaluation of Soil Vacuum Extraction Application," in *Proceedings, 4th National Outdoor Action Conference on Aquifer Restoration, Ground Water Monitoring and Geophysical Methods, May 14–17, 1990, Las Vegas, NV*, p. 587.
30. J. M. Rodríguez-Maroto and D. J. Wilson, "Soil Cleanup by In Situ Aeration. VII. High-Speed Modeling of Diffusion Kinetics," *Sep. Sci. Technol.*, *26*, 743 (1991).
31. J. M. Rodríguez-Maroto, C. Gómez-Lahoz, and D. J. Wilson, "Mathematical Modeling of SVE: Effects of Diffusion Kinetics and Variable Permeabilities," in *Proceedings,*

Symposium on Soil Venting, April 29–May 1, 1991, Houston, TX, D. DiGiulio, project officer, U.S. EPA Report EPA/600/R-92/174, 1992, p. 103.

32. C. Gómez-Lahoz, R. A. García-Delgado, F. García-Herruzo, J. M. Rodríguez-Maroto, and D. J. Wilson, *Extraccion a Vacio de Contaminantes Organicos del Suelo. Fenomenos de No-Equilibrio*, Presented at the III Congreso de Ingeniería Ambiental, Proma '93, Bilbao, Spain.
33. C. Gómez-Lahoz, J. M. Rodríguez-Maroto and D. J. Wilson, "Biodegradation Phenomena during Soil Vapor Extraction: A High-Speed Non-Equilibrium Model," *Sep. Sci. Technol.*, *29*, 429 (1994).
34. D. J. Wilson, C. Gómez-Lahoz, and J. M. Rodríguez-Maroto, "Soil Cleanup by In Situ Aeration. XVI. Solution and Diffusion in Mass Transport-Limited Operation and Calculation of Darcy's Constants," *Ibid.*, *29*, 1133 (1994).
35. C. Gómez-Lahoz, J. M. Rodríguez-Maroto, and D. J. Wilson, "Soil Cleanup by In Situ Aeration. XVII. Field Scale Model with Distributed Diffusion," *Ibid.*, *29*, 1251 (1994).
36. W. R. Smythe, *Static and Dynamic Electricity*, 4th ed., McGraw-Hill, New York, 1953.

Received by editor November 19, 1993